Cross-Electron-Transfer Reactions of the $[Cu^{II/I}(bite)]^{2+/+}$ Redox Couple

Boping Xie,[†] Lon J. Wilson,[‡] and David M. Stanbury*,[†]

Department of Chemistry, Auburn University, Alabama 36849, and Department of Chemistry and Laboratory for Biochemical and Genetic Engineering, Rice University, MS 60, P.O. Box 1892, Houston, Texas 77251-1892

Received April 4, 2000

A series of outer-sphere cross-electron-transfer reactions involving the $[Cu(bite)]^{2+/+}$ redox couple has been investigated in acetonitrile at 25 °C. In this complex, the bite ligand is a macrocyclic N_2S_2 ligand with a 2,2′-biphenyl moiety as its backbone. The reaction of $[Cu^{II}(bite)]^{2+}$ with $[Ru(hfac)_3]^-$ produces $[Cu^{I}(bite)]^+$ and $[Ru(hfac)_3]$ reversibly with $K = 1.9$. The rate law is second order in both directions, with a rate constant of $(8.22 \pm 0.27) \times 10^2$ M^{-1} s^{-1} in the forward direction. Rate constants were also obtained for the irreversible reactions of three Co(II) clathrochelates with $[Cu(bite)]^{2+}$. The oxidation of $[Cu(bite)]^+$ by $[Fe(bpy)_3]^{3+}$ was studied in order to obtain a rate constant for oxidation as well as reduction. Application of the Marcus cross relationship to these rate constants gives apparent self-exchange rate constants that are reasonably consistent yet unusually low, with an average value of 1.0×10^{-2} M^{-1} s^{-1}. The self-consistence of the apparent self-exchange rate constants implies that all of the cross reactions proceed through the same intermediate, and hence, the outer-sphere self-exchange reaction should have a second-order rate law with $k = 1.0 \times 10^{-2}$ M^{-1} s^{-1}. The much faster first-order self-exchange process reported previously for the $[Cu(bite)]^{2+/+}$ couple in acetone implies a more efficient mechanism for the self-exchange reaction than for the cross reactions, such as an inner-sphere mechanism. Cyclic voltammograms of $[Cu(bite)]^{n+}$ are strongly sensitive to the nature of the working electrode, thus precluding the use of these data in interpreting the homogeneous redox kinetics.

Introduction

Copper ions in metalloproteins play important roles in most living organisms.[1] Many attempts have been made to generate low-molecular-weight model compounds that duplicate the properties of the type-I copper center found in the blue copper proteins.[2] In addition, the properties of many other low-molecular-weight copper complexes have been examined to determine to what extent both the kinetic and thermodynamic properties of the Cu(II/I) redox couple are dependent upon geometry and coordination atoms. The more interesting studies in this regard are the investigations of copper complexes that are coordination number invariant (CNI).[3,4]

The new macrocyclic compound $[Cu^{I}(bite)](BF_4)$ (bite = biphenyldiimino dithioether) was synthesized from template condensation of 2,2′-diaminobiphenyl, 1,4-bis(2-formylphenyl)-dithiabutane, and copper(II) tetrafluoroborate, as shown here.[5]

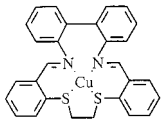

= $[Cu(bite)]^{n+}$

$[Cu^{II/I}(bite)]^{2+/+}$ is of particular interest because it is CNI, and the primary coordination environments of both oxidation states are the same in solution as in the solid as judged from EXAFS, X-ray crystallography, NMR spectroscopy, and electronic spectroscopy. In addition, it is the first example of a Cu(I) coordination compound that is both "tetrahedral" and macrocyclic with an N_2S_2 donor atom set. The Cu(II) coordination structure shows similar features with the exception that the configuration at the sulfur atoms or the twist of the biphenyl backbone is inverted relative to the Cu(I) complex, which leads to an approximately square-planar metal center as is typical of Cu(II).[5] Weak axial interactions between $[Cu(bite)]^{2+}$ and the BF_4^- counterions are also seen in the crystal structure, but there is no evidence that such interactions affect the solution chemistry.

For the $[Cu^{II/I}(bite)]^{2+/+}$ couple, a question relating to its electron-transfer mechanism is as follows: should the small, restricted geometry difference between the two oxidation states lead to rapid or slow electron-transfer kinetics? The present thinking about the electron-transfer reactivity of copper proteins is mainly based on the "entatic state hypothesis", which states that structural rigidity (without change in coordination number) is essential for fast electron transfer.[6] In a contrasting view, the "square-scheme" emphasizes the role of structural change in gating of electron-transfer reactivity; that is, that active sites may take advantage of changes in coordination geometry (with potential change in coordination number) to limit the rates of electron transfer.[7] In our original report on the $[Cu^{II/I}(bite)]^{2+/+}$ couple, electron self-exchange kinetics measured by ^1H NMR

* To whom correspondence should be addressed.
† Auburn University.
‡ Rice University.

(1) *Copper Proteins*; Spiro, T. G., Ed.; Wiley: New York, 1981; pp 1−363.
(2) Casella, L.; Guilotti, M.; Pintar, A.; Pinciroli, F.; Viganó, R.; Zanello, P. *J. Chem. Soc., Dalton Trans.* **1989**, 1161−1169.
(3) Goodwin, J. A.; Stanbury, D. M.; Wilson, L. J.; Eigenbrot, C. W.; Scheidt, W. R. *J. Am. Chem. Soc.* **1987**, *109*, 2979−2991.
(4) Goodwin, J. A.; Wilson, L. J.; Stanbury, D. M.; Scott, R. A. *Inorg. Chem.* **1989**, *28*, 42−50.
(5) Flanagan, S.; Dong, J.; Haller, K.; Wang, S.; Scheidt, W. R.; Scott, R. A.; Webb, T. R.; Stanbury, D. M.; Wilson, L. J. *J. Am. Chem. Soc.* **1997**, *119*, 8857−8868.
(6) Williams, R. J. P. *Eur. J. Biochem.* **1995**, *234*, 363−381.
(7) Martin, M. J.; Endicott, J. F.; Ochrymowycz, L. A.; Rorabacher, D. B. *Inorg. Chem.* **1987**, *26*, 3012−3022.

10.1021/ic000358w CCC: $20.00
Published on Web 06/08/2001

line broadening of $[Cu^{I}(bite)]^{+}$ in the presence of $[Cu^{II}(bite)]^{2+}$ revealed an overall first-order process (rate of exchange = $k_{ex}[Cu^{I}(bite)^{+}]$) with a rate constant of 21.7 (1.9) s^{-1} at 295 K in acetone-d_6.[5] Thus, it is apparently the first example of fully gated electron transfer from small-molecule copper(I). Although we have now modified our interpretation as described below, this gating was rationalized in terms of a mechanism with the first step being the rate-limiting isomerization of $[Cu^{I}(bite)]^{+}$ from its stable pseudo-tetrahedral conformer (as found crystallographically) to a high-energy square-planar conformer (resembling $[Cu^{II}(bite)]^{2+}$).

In the current research, we report direct measurements of electron-transfer kinetics involving both oxidation and reduction cross reactions for this system by use of UV−vis stopped-flow methods. The reduction reactions of $[Cu^{II}(bite)]^{2+}$ were conducted with a series of cobalt(II) clathrochelates and the tris(hexafluoroacetylacetonato)ruthenium(II) complex, while the oxidation of $[Cu^{I}(bite)]^{+}$ was studied with tris(2,2′-bipyridyl)iron(III). These reagents have been thoroughly studied and are all well-known to react through outer-sphere electron-transfer mechanisms.[8−18] Interestingly, the $[Cu(bite)]^{2+/+}$ self-exchange rate constants obtained by applying the Marcus cross relationship to the experimentally determined cross-reaction rate constants are relatively constant for both oxidation and reduction reactions, show unusually slow electron-transfer kinetics, and reveal a difference in mechanism between the cross reactions and the self-exchange reaction.

Experimental Section

Materials. All materials were used as received unless otherwise noted. All solvents were reagent grade or better. Acetonitrile (Fisher) for electronic spectra, equilibrium constants, and kinetic and electrochemical measurements was distilled under N_2 from CaH_2 and stored in a glovebox (controlled atmosphere glovebox, LABCONCO corporation) under nitrogen.

Methanol, acetone, dichloromethane, benzene, ethyl acetate, dimethylformamide, 2-propanol, hexane, methylene chloride, and sodium hydroxide were reagent grade from Fisher. Pentane, tetrahydrofuran, tetraethylammonium tetrafluoroborate, 1-butaneboronic acid, 1,2-cyclohexanedione dioxime, phenylboric acid, nitrosonium tetrafluoroborate, ruthenium(III) chloride hydrate, 1,1,1,5,5,5-hexafluoro-2,4-pentanedione, hydrogen peroxide (30 wt % solution in water), silica gel (200−400 mesh, 60 Å) for column chromatography, 2,2′-dipyridyl, iron(II) tetrafluoroborate hexahydrate, and ammonium tetrafluoroborate were purchased from Aldrich. Absolute ethyl alcohol came from Florida Distillers Co. Dimethylglyoxime was purchased from J. T. Baker. Ferrocene (Aldrich) used for electrochemical studies was sublimed.

The supporting electrolyte, Et_4NBF_4 (Aldrich), used in electronic spectra, equilibrium constants, and kinetic and electrochemical measurements was recrystallized three times from a mixture of methanol and hexane (4:1) and dried under vacuum at 95 °C in an Abderhalden pistol.

Preparation of the Copper Complexes. 2,2′-Diaminobiphenyl-1,4-bis(2-formylphenyl)-1,4-dithiabutanecopper(I) tetrafluoroborate, $[Cu^{I}(bite)](BF_4)$, and its copper(II) tetrafluoroborate, $[Cu^{II}(bite)](BF_4)_2$, were synthesized as described previously.[5]

Preparation of the Cobalt Complexes. The cobalt compounds, $[Co^{II}((nox)_3(BC_6H_5)_2)]$, $[Co^{II}((nox)_3(BC_4H_9)_2)]$, $[Co^{II}((dmg)_3(BC_4H_9)_2)]$, $[Co^{III}((nox)_3(BC_6H_5)_2)]BF_4$ were available from a prior study.[19] These are clathrochelates in which the ligand moiety cyclohexanedionedioximate is abbreviated as nox, while dimethylglyoximate is abbreviated as dmg.

Preparation of the Ruthenium Complexes. The ruthenium compounds $K[Ru^{II}(hfac)_3]$ and $[Ru^{III}(hfac)_3]$ (hfac = hexafluoroacetylacetonato) were prepared as described in the literature.[12] Ruthenium(III) chloride hydrate (1.00 g) was dissolved in a mixture of 50 mL of water and 50 mL of ethanol. The solution was refluxed for 4 h. The ligand, 1,1,1,5,5,5-hexafluoro-2,4-pentanedione (3.31 g), was added to the solution, and the mixture was refluxed for 2 h. The mixture was cooled, potassium hydrogencarbonate (2.50 g) was added to the mixture, and the mixture was refluxed for another 1 h. The procedure was repeated until the color of the mixture gradually turned purple. The solution was concentrated to 50 mL by rotary evaporation and was dried under a vacuum. The precipitate was extracted with benzene (20 mL). The residue of the benzene extraction was extracted with acetone (50 mL). The acetone extract was passed through a column of silica gel (200−400 mesh, 60 Å). The eluant was evaporated to dryness. The Ru(II) product was washed with benzene and dried under vacuum.

The $K[Ru^{II}(hfac)_3]$ (0.80) was suspended in water (60 mL), and benzene (60 mL) was added to the suspension. HCl (4 M, 1 mL) was added, and 30 wt % solution in water of hydrogen peroxide (2 mL) was added dropwise to the mixture with stirring. The oxidized complex $[Ru^{III}(hfac)_3]$ was extracted into benzene (100 mL). The benzene phase was separated and evaporated to dryness. The residue was again extracted with hexane (100 mL). The Ru(III) product was obtained by rotary evaporation to remove hexane and drying under vacuum. The UV−vis spectra of both ruthenium compounds were consistent with the literature.[12]

Preparation of the Iron Complexes. $Fe(BF_4)_2 \cdot 6H_2O$ (5.00 g, 0.015 mol) was dissolved in 300 mL of water; (0.045 mol, 7.03 g) 2,2′-dipyridyl (bpy) was added to the solution. The solution was stirred for 1 h. Then NH_4BF_4 (3.14 g) was added to the solution to precipitate $[Fe^{II}(bpy)_3](BF_4)_2$. The mixture was filtered and washed with water. The final product was dried overnight under a vacuum. Yield: 9.42 g (90%).

A 1.5 mM solution of $[Fe^{III}(bpy)_3](BF_4)_3$ in acetonitrile with 0.1 M Et_4NBF_4 was made by electrochemically oxidizing 1.5 mM $[Fe^{II}(bpy)_3](BF_4)_2$ in acetonitrile with 0.1 M Et_4NBF_4 using a BAS SP-2 Synthetic potentiostat with an applied potential of 1.40 V. A cylindrical platinum mesh was used as the working electrode. The reference electrode was an aqueous saturated silver/silver chloride electrode. It was dipped into a tube filled with 0.1 M Et_4NBF_4 in acetonitrile, and the tube with fritted glass bottom was inserted into the working solution. The platinum mesh auxiliary electrode was inserted into acetonitrile with 0.1 M Et_4NBF_4 and was separated from the main compartment by a fritted glass disk. The cell compartment was flushed by nitrogen gas, which was passed through the concentrated sulfuric acid and then acetonitrile with 0.1 M Et_4NBF_4, before and during the electrolysis. The UV−vis spectra of both iron compounds were consistent with literature.[20]

Analytical Electrochemistry. A BAS-100 electrochemical analyzer with a Pt wire auxiliary electrode, an aqueous saturated silver/silver chloride reference electrode, and a 1.8 mm diameter Pt disk working electrode were used for the cyclic voltammetry measurements. Potentials are reported relative to ferrocene/ferrocenium. The surface of the working electrode was cleaned prior to each experiment by polishing with alumina followed by sonication. The electrode was preconditioned by electrolysis at −2 V in acetonitrile with 0.01 or 0.1 M Et_4NBF_4 for 1 min.[8] In certain experiments, the working electrode was glassy carbon

(8) Borchardt, D.; Pool, K.; Wherland, S. *Inorg. Chem.* **1982**, *21*, 93−97.
(9) Borchardt, D.; Wherland, S. *Inorg. Chem.* **1986**, *25*, 901−905.
(10) Anderson, K. A.; Wherland, S. *Inorg. Chem.* **1991**, *30*, 624−629.
(11) Wherland, S. *Coord. Chem. Rev.* **1993**, *123*, 169−199.
(12) Endo, A.; Kajitani, M.; Mukaida, M.; Shimizu, K.; Satô, G. P. *Inorg. Chim. Acta* **1988**, *150*, 25−34.
(13) Patterson, G. S.; Holm, R. H. *Inorg. Chem.* **1972**, *11*, 2285−2288.
(14) Nielson, R. M.; McManis, G. E.; Safford, L. K.; Weaver, M. J. *J. Phys. Chem.* **1989**, *93*, 2152−2157.
(15) McManis, G. E.; Nielson, R. M.; Gochev, A.; Weaver, M. J. *J. Am. Chem. Soc.* **1989**, *111*, 5533−5541.
(16) Nelsen, S. F.; Wang, Y.; Ramm, M. T.; Accola, M. A.; Pladziewicz, J. R. *J. Phys. Chem.* **1992**, *96*, 10654−10658.
(17) Lever, A. B. P. *Inorg. Chem.* **1990**, *29*, 1271−1285.
(18) Chan, M.-S.; Wahl, A. C. *J. Phys. Chem.* **1978**, *82*, 2542−2549.
(19) Xie, B.; Elder, T.; Wilson, L. J.; Stanbury, D. M. *Inorg. Chem.* **1999**, *38*, 12−19.
(20) Schilt, A. A. *Analytical Applications of 1,10-Phenanthroline and Related Compounds*; Pergamon: New York, 1969.

or gold instead of platinum. Scan rates ranged from 30 to 400 mV s^{-1}. Four sweep segments were usually performed. The cyclic voltammetry investigations were carried out at ambient temperature (24 ± 1 °C). All solutions were made in acetonitrile with 0.01 M Et_4NBF_4 in the glovebox under nitrogen. No attempt was made to exclude air during the electrochemical measurements. Digital simulations of the CVs were performed with the computer program DigiSim (BAS).

Spectrophotometric Equilibrium Constant. The equilibrium constant for the reaction between $[Cu^{II}(bite)](BF_4)_2$ and $K[Ru^{II}(hfac)_3]$ was obtained by spectrophotometry using a Hewlett-Packard 8453 UV−vis spectrophotometer with quartz cells of 1.00-cm path length. The solutions were equilibrated in cuvettes thermostated at 25 °C. All solutions of $[Cu^{II}(bite)](BF_4)_2$ (initial concentrations: 0.079, 0.100, and 0.134 mM) and $K[Ru^{II}(hfac)_3]$ (initial concentration: 0.010 mM) were made in acetonitrile with 0.01 M Et_4NBF_4 in the glovebox under nitrogen. Ruthenium(II) solution (1.20 mL) was added into a cell by a 2.00-ml syringe, and the cell was then sealed with a stopcock. The needle of a syringe with 1.20 mL copper solution was inserted through a rubber septum at the other end of the stopcock. Then the whole system was moved from the glovebox to the UV−vis apparatus. The Cu/Ru mixtures were prepared at the UV−vis instrument with exclusion of air by means of this setup. The progress of the reaction was monitored at 376 nm, which corresponds to the absorption peak of the Ru(III) complex.

Cross-Exchange Kinetics. The kinetics studies were performed on an OLIS rapid scanning monochromator (RSM 1000) with dual-beam UV−vis recording. The instrument obtains one scan per ms at 1 nm resolution, with a quartz cell of 1.7 cm path length. The temperature was maintained at 25 °C with a Forma Scientific 2095 bath & circulator. All solutions of $K[Ru^{II}(hfac)_3]$, $[Cu^{II}(bite)](BF_4)_2$, $[Ru^{III}(hfac)_3]$, $[Co^{II}((nox)_3(BC_6H_5)_2)]$, $[Co^{II}((dmg)_3(BC_4H_9)_2)]$, and $[Co^{II}((nox)_3(BC_4H_9)_2)]$ were made in acetonitrile with 0.01 M Et_4NBF_4 in a glovebox under nitrogen. Solutions of $[Cu^{II}(bite)](BF_4)_2$ and $[Co^{II}((nox)_3(BC_4H_9)_2)]$ were also made in acetonitrile with 0.1 M Et_4NBF_4, and all solutions of $[Cu^{I}(bite)](BF_4)$ and $[Fe^{II}(bpy)_3](BF_4)_2$ were made in acetonitrile with 0.1 M Et_4NBF_4 in the glovebox under nitrogen. In all cases there was at least a 10-fold excess of $[Cu^{II}(bite)](BF_4)_2$ over the selected counter-reagents except there was at least a 10-fold excess of $[Fe^{III}(bpy)_3](BF_4)_3$ over $[Cu^{I}(bite)](BF_4)$. All stock solutions of Cu(II), Cu(I), Co(II), and Ru(II) were prepared by weight. The stock solution of $[Fe^{III}(bpy)_3](BF_4)_3$ was made immediately before use by bulk electrolysis of $[Fe^{II}(bpy)_3](BF_4)_2$.

For the reactions of $[Cu^{II}(bite)]^{2+}$ with the three Co(II) compounds, the spectral changes due to the decay of the absorbance of Cu(II) were monitored in the visible region (550−750 nm). In general, the initial Co(II) concentrations were 0.010 mM, and a series of kinetic runs was performed under pseudo-first-order conditions with [Cu(II)] varying from 0.1 to 0.3 or 0.4 mM.

For the pseudo-first-order reaction of $[Cu^{II}(bite)]^{2+}$ with $[Ru^{II}(hfac)_3]^-$, the initial concentrations of $[Cu^{II}(bite)](BF_4)_2$ were: 0.025, 0.050, 0.075, 0.100, 0.125, 0.150, and 0.175 mM. A solution was made containing $K[Ru^{II}(hfac)_3]$ (initial concentration: 0.005 mM) and $[Cu^{I}(bite)](BF_4)$ (initial concentration: 0.050 mM) in acetonitrile with 0.01 M Et_4NBF_4 in the glovebox under nitrogen. The spectral changes due to the increase of the absorbance of Ru(III) were monitored in the UV−vis region (300−500 nm).

For the pseudo-first-order reaction of $[Cu^{I}(bite)]^{+}$ with $[Fe^{III}(bpy)_3]^{3+}$, the initial concentration of $[Cu^{I}(bite)](BF_4)$ was 0.025 mM, and the initial concentrations of $[Fe^{III}(bpy)_3](BF_4)_3$ were: 0.250, 0.375, 0.500, 0.625, and 0.750 mM, in acetonitrile with 0.1 M Et_4NBF_4. The spectral changes due to the increase of the absorbance of Fe(II) were monitored in the visible region (440−660 nm).

All of the kinetics were obtained as multiwavelength data sets and analyzed using the global fitting subroutine of the RSM 1000 system (version 5.8.3) to obtain values of the pseudo-first-order rate constants, k_{obs}. Some of the runs were verified by single wavelength fits. Values of the pseudo-first-order rate constants are given as Supporting Information in Tables S-1−S-6.

A nonlinear-least-squares program was used to fit rate laws to the values of k_{obs}, with weighting as the inverse square of k_{obs}.[21]

Results

In this work, we report on the reduction of $[Cu^{II}(bite)]^{2+}$ by three different Co(II) clathrochelate complexes and the tris(hexafluoroacetylacetonato)ruthenium(II) complex, as indicated in reactions 1−4. Also we describe the oxidation of $[Cu^{I}(bite)]^{+}$ by tris(2,2′-bipyridyl)iron(III), as indicated in reaction 5.

$$[Cu^{II}(bite)]^{2+} + [Co^{II}((nox)_3(BC_6H_5)_2)] \rightleftharpoons [Cu^{I}(bite)]^{+} + [Co^{III}((nox)_3(BC_6H_5)_2)]^{+} \quad k_{12}, k_{21} \quad (1)$$

$$[Cu^{II}(bite)]^{2+} + [Co^{II}((nox)_3(BC_4H_9)_2)] \rightleftharpoons [Cu^{I}(bite)]^{+} + [Co^{III}((nox)_3(BC_4H_9)_2)]^{+} \quad k_{12}, k_{21} \quad (2)$$

$$[Cu^{II}(bite)]^{2+} + [Co^{II}((dmg)_3(BC_4H_9)_2)] \rightleftharpoons [Cu^{I}(bite)]^{+} + [Co^{III}((dmg)_3(BC_4H_9)_2)]^{+} \quad k_{12}, k_{21} \quad (3)$$

$$[Cu^{II}(bite)]^{2+} + [Ru^{II}(hfac)_3]^{-} \rightleftharpoons [Cu^{I}(bite)]^{+} + [Ru^{III}(hfac)_3] \quad k_{12}, k_{21} \quad (4)$$

$$[Cu^{I}(bite)]^{+} + [Fe^{III}(bpy)_3]^{3+} \rightleftharpoons [Cu^{II}(bite)]^{2+} + [Fe^{II}(bpy)_3]^{2+} \quad k_{21}, k_{12} \quad (5)$$

Note that with the exception of reaction 4, all of the reactions proceed to completion; however, they are written as reversible processes here in order to facilitate discussion.

Cyclic Voltammetric Studies. In cyclic voltammetric measurements on each system, the potential range was limited to include only that interval in which the complex itself was being oxidized and reduced. The cyclic voltammograms of the compounds $[Co^{III/II}((nox)_3(BC_4H_9)_2)]^{+/0}$, $[Co^{III/II}((nox)_3(BC_6H_5)_2)]^{+/0}$, $[Co^{III/II}((dmg)_3(BC_4H_9)_2)]^{+/0}$, $[Ru^{III/II}(hfac)_3]^{0/-}$, and $[Fe^{III/II}(bpy)_3]^{3+/2+}$ in acetonitrile at ambient temperature (24 ± 1 °C) show quasi-reversible waves with $\Delta E_{p/p}$ values significantly greater than 59 mV and, with the exception of $[Co^{III/II}((dmg)_3(BC_4H_9)_2)]^{+/0}$, are in good agreement with prior reports.[9,13,17] In the case of $[Co^{III/II}((dmg)_3(BC_4H_9)_2)]^{+/0}$, there are two prior reports on $E_{1/2}$ that inexplicably differ from each other by 131 mV after correction to a common reference electrode;[9,22] our $E_{1/2}$ value lies approximately midway between those prior reports. Although we erred previously in claiming good agreement with prior work on this compound,[19] we encountered no difficulties in handling this compound and we believe our results to be correct. For the Co(III/II) couples, the cyclic voltammetry behaviors in acetonitrile with 0.01 M Et_4NBF_4 at ambient temperature (24 ± 1 °C) are essentially the same as those described previously,[19] where the results were obtained at the higher ionic strength of 0.1 M Et_4NBF_4. For the $[Ru^{III/II}(hfac)_3]^{0/-}$ and $[Fe^{III/II}(bpy)_3]^{3+/2+}$ couples, the anodic and cathodic waves are symmetric; the $\Delta E_{p/p}$ values and the $E_{1/2}$ values are independent of scan rate, as expected for fast electrode kinetics. For all of these systems the $E_{1/2}$ values are good measures of the formal potential E_f. A summary of the results is given in Table 1.

(21) Moore, R. H.; Zeigler, R. K. *LSTSQR*, 1959, Los Alamos National Laboratory, Los Alamos, NM.
(22) Nielson, R. M.; Weaver, M. J. *J. Electroanal. Chem.* **1989**, *260*, 15−24.

Table 1. Cyclic Voltammetry Results: Half-Wave Potentials (E_{12}) and Peak-to-Peak Separations ($\Delta E_{p/p}$)[a]

redox couple	$E_{1/2}$,[b] mV	$\Delta E_{p/p}$,[b] mV	υ,[c] mV/s
$[Cu^{II/I}(bite)]^{2+/+}$ [d]	324	232	50
$[Ru^{III/II}(hfac)_3]^{-/0}$	300	84	40
$[Co^{III/II}((nox)_3(BC_4H_9)_2)]^{0/+}$	−291	94	30
$[Co^{III/II}((nox)_3(BC_6H_5)_2)]^{0/+}$	−184	86	100
$[Co^{III/II}((dmg)_3(BC_4H_9)_2)]^{0/+}$	−318	80	30
$[Fe^{III/II}(bpy)_3]^{3+/2+}$ [e]	660	69	100
$[Fe^{III/II}(cp)_2]^{+/0}$	0	63	100

[a] In acetonitrile with 0.01 M Et_4NBF_4 at 25 °C, Pt working electrode. [b] Potentials vs ferrocene/ferrocenium. [c] Scan rate. [d] Anodic wave poorly resolved. [e] In acetonitrile with 0.1 M Et_4NBF_4 at ambient temperature (24 ± 1 °C).

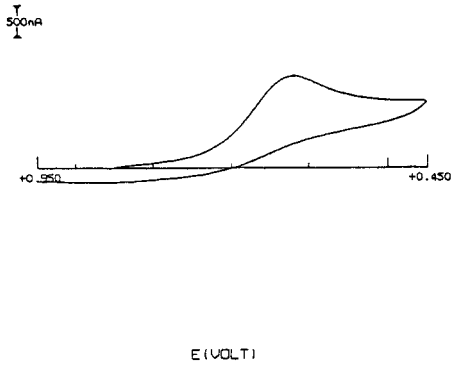

Figure 1. Single-scan cyclic voltammogram of 0.5 mM $[Cu^{II}(bite)]^{2+}$ in acetonitrile with 0.01 M Et_4NBF_4 at ambient temperature (24 ± 1 °C). Pt working electrode: scan range 0.450−0.950 V at a scan rate of 0.05 V s^{-1}.

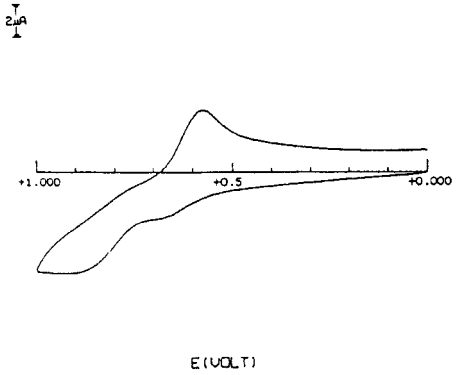

Figure 2. Single-scan cyclic voltammogram of 0.5 mM $[Cu^{I}(bite)]^{+}$ in acetonitrile with 0.01 M Et_4NBF_4 at ambient temperature (24 ± 1 °C). Pt working electrode: scan range 0.000−1.000 V at a scan rate of 0.20 V s^{-1}.

For $[Cu(bite)]^{n+}$, however, the cyclic voltammograms are clearly irreversible. At glassy carbon and gold working electrodes the CVs were quite ill-defined. Well-resolved waves were obtained at platinum, and all subsequent results are reported with that electrode. For $[Cu^{II}(bite)]^{2+}$, a well-developed cathodic wave is observed in acetonitrile with 0.01 M Et_4NBF_4 at ambient temperature (24 ± 1 °C), as shown in Figure 1. For $[Cu^{I}(bite)]^{+}$ under the same conditions, a single cathodic peak was always observed. At the same time, an anodic peak at more positive potential (around 920 mV) was always observed. When the scan rate was decreased from 600 mV s^{-1} to less than 400 mV s^{-1}, an additional oxidation wave/shoulder was detected at less positive potentials (around 680 mV), as shown in Figure 2. However, an analogous behavioral pattern was not observed for $[Cu^{II}(bite)]^{2+}$ under the same conditions as with $[Cu^{I}(bite)]^{+}$. In view of the sensitivity of the CV results to the nature of the working electrode, it is reasonable to assign these electrochemical features to adsorption phenomena. Despite this conclusion, it is interesting to note that we have been able to achieve a reasonably accurate simulation of Figure 2 by use of an electrochemical square scheme.

Equilibrium Spectrophotometry. The value of the equilibrium quotient for reaction 4 ($[Ru(hfac)_3]^{0/-}$) in acetonitrile with 0.01 M Et_4NBF_4 at 25 °C was obtained by spectrophotometry. UV−vis data for related compounds, which were used to obtain the equilibrium constant for the reaction 4, are shown in Table 2. The $[Cu^{I}(bite)]^{+}$ and $[Ru^{II}(hfac)_3]^{-}$ compounds are very stable in acetonitrile with 0.01 M Et_4NBF_4, and there is no net reaction between $[Cu^{I}(bite)]^{+}$ and $[Ru^{II}(hfac)_3]^{-}$. The $[Cu^{I}(bite)]^{+}$ compound has a tailing absorption in the UV but no absorption peak in the 300−800 nm wavelength range. The peak at 376 nm for Ru(III) was monitored during the measurements of the equilibrium constants. Reaction 4 occurs with an increase of absorbance at 376 nm for $[Ru^{III}(hfac)_3]$, and it proceeds to an equilibrium position as indicated. Upon addition of Ru(II), the peak at 376 nm, corresponding to the absorption peak of the Ru(III) complex, first increased and then stabilized with the progress of the reaction. For reaction 4, the absorbance of the solution at any time is given by eq 6

$$A/l = [Cu(II)]\epsilon_{Cu(II)} + [Ru(II)]\epsilon_{Ru(II)} + [Cu(I)]\epsilon_{Cu(I)} + [Ru(III)]\epsilon_{Ru(III)} \quad (6)$$

where A is the absorbance, l is the path length, and ϵ is the pertinent molar absorptivity. The overall absorbance change in the reaction is indicated as ΔA, such that

$$\Delta A = A_o - A_\infty \quad (7)$$

where A_o and A_∞ represent the absorbance of the reaction at the time of initiation and at equilibrium, respectively. Substitution of eq 6 into eq 7 leads to

$$\Delta A/l = X(\epsilon_{Cu(II)} + \epsilon_{Ru(II)} - \epsilon_{Cu(I)} - \epsilon_{Ru(III)}) \quad (8)$$

where X represents $[Cu(II)]_o - [Cu(II)]_\infty$. Rearrangement of eq 8 and use of the spectral data in Table 2 at 376 nm with a 1.0 cm path length give eq 9:

$$X = \Delta A/(-4.81 \times 10^3\ M^{-1}) \quad (9)$$

In general, the equilibrium constant is given by

$$K_{12} = ([Cu(I)]_o + X)([Ru(III)]_o + X)/\{([Cu(II)]_o - X)([Ru(II)]_o - X)\} \quad (10)$$

Values of the equilibrium constant were thus measured under three different sets of initial conditions as shown in Table 3. The average value of K_{12} for reaction 4 is 1.90. This value was further verified by kinetic measurements in the next section.

Cross-Exchange Kinetics. The electron-transfer kinetics of $[Cu^{II/I}(bite)]^{2+/+}$ were studied by reducing the Cu(II) complex and by oxidizing the Cu(I) complex. Favorable characteristics for the reducing and oxidizing agents include (1) a constrained coordination geometry that promotes an outer-sphere electron-transfer process; (2) an established self-exchange rate constant; (3) a large molar absorptivity value for reactants or products that could by used to monitor the reaction progress; and (4) a formal potential value capable of reducing Cu(II) or of oxidizing Cu(I). Three different cobalt compounds and one ruthenium

Table 2. UV−Vis Spectral Features in Acetonitrile with 0.01 M Et_4NBF_4 at 25 °C

species[a]	λ_{1max} (nm)	ϵ_{1max} ($M^{-1}\,cm^{-1}$)	λ_{2max} (nm)	ϵ_{2max} ($M^{-1}\,cm^{-1}$)	λ_{3max} (nm)	ϵ_{3max} ($M^{-1}\,cm^{-1}$)	ϵ_{376}[b] ($M^{-1}\,cm^{-1}$)
$[Cu^{II}(bite)]^{2+}$	406	6.46×10^3	658	1.47×10^3			4.29×10^3
$[Cu^{I}(bite)]^{+}$[c]							2.79×10^3
$[Ru^{II}(hfac)_3]^-$	233	1.25×10^4	288	2.43×10^4	529	1.81×10^4	1.33×10^3
$[Ru^{III}(hfac)_3]$	288	1.26×10^4	376	7.64×10^3	529	3.78×10^3	7.64×10^3
$[Fe^{II}(bpy)_3]^{2+}$	522	9.26×10^4					

[a] Ligand abbreviations: bite, 2,2′-diaminophenyl-1,4-bis(2-formylphenyl)-1,4-dithiabutane; hfac, hexafluoroacetylacetonate ion. [b] The Ru(III) peak at 376 nm was chosen for the measurements of the equilibrium constants. [c] This compound has no absorption peak in the 300−800 nm wavelength range.

Table 3. Spectrophotometric Equilibrium Constant for the Reduction of $[Cu^{II}(bite)]^{2+}$ by $[Ru^{II}(hfac)_3]^-$[a]

$[Cu^{II}(bite)^{2+}]_{init}$ (mM)	$A_{0,cal}$	$A_{\infty,exp}$	K_{12}
7.90×10^{-2}	0.3518	0.3974	2.486
1.00×10^{-1}	0.4418	0.4867	1.458
1.34×10^{-1}	0.5875	0.6336	1.756
			$K_{12,avg} = 1.90 \pm 0.53$

[a] At 25 °C in CH_3CN with $[Ru^{II}(hfac)_3^-]_{init} = 1.00 \times 10^{-2}$ mM, $\mu = 0.01$ M (Et_4NBF_4), the peak at 376 nm observed, the path length = 1 cm, and K_{12} calculated by use of eq 10.

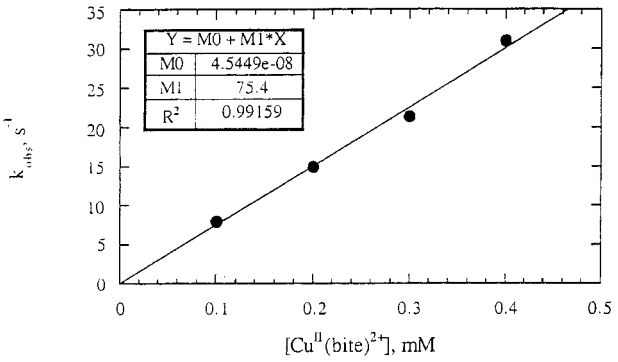

Figure 3. Pseudo-first-order rate constants for the reaction of $[Co^{II}((nox)_3(BC_4H_9)_2)]$ with excess $[Cu^{II}(bite)]^{2+}$ in acetonitrile with 0.01 M Et_4NBF_4 at 25 °C. $[Co^{II}]_0 = 0.010$ mM.

compound were used as a reducing agents, as shown in reactions 1−4, respectively. Tris(2,2′-bipyridyl)iron(III) was used as an oxidizing agent, as shown in reaction 5. Conditions were selected so as to drive the reactions to at least 95% completion, such that the reverse reactions could be safely neglected except reaction 4 (that of Ru(II)). The reactions were studied under pseudo-first-order conditions. Repetitive-scan studies showed the clean consumption of reactants, with no evidence for the buildup of intermediates.

Preliminary study also indicated that the reduction of $[Cu^{II}(bite)]^{2+}$ by ferrocene is fairly rapid on the stopped-flow time scale.

(1) Reduction Kinetics Using $[Co^{II}((nox)_3(BC_6H_5)_2)]$, $[Co^{II}((nox)_3(BC_4H_9)_2)]$, and $[Co^{II}((dmg)_3(BC_4H_9)_2)]$. Reactions 1−3 were monitored by following the loss of Cu(II) at 658 nm. The kinetics were studied under pseudo-first-order conditions with at least a 10-fold excess of Cu(II) at $\mu = 0.01$ M. For all three reactions the integrated rate equation is of the form

$$\ln([Co^{II}]_o/[Co^{II}]_t) = k_{obs}t \qquad (11)$$

where $[Co^{II}]_o$ and $[Co^{II}]_t$ represent the concentrations of the Co(II) complex at the time of reaction initiation and at any time, t, respectively. A representative plot of the kinetic data is shown in Figure 3 for reaction 2 ($Co^{II}((nox)_3(BC_4H_9)_2)$), while analogous plots for reactions 1 and 3 are shown in Figures S-1 and S-2 (Supporting Information). The linear dependence of k_{obs} on $[Cu(II)]_o$ as in eq 12

$$k_{obs} = k_{12}[Cu^{II}]_o \qquad (12)$$

indicates that the reactions obey second-order kinetics conforming to the overall differential rate expression

$$-d[Co^{II}]/dt = k_{12}[Cu^{II}][Co^{II}] \qquad (13)$$

where $[Co^{II}]$ represents the concentration of the corresponding cobalt complex and $[Cu^{II}]$ represents the concentration of the copper(II) complex. At least five determinations of k_{obs} with good reproducibility were obtained at each concentration. Average values of k_{obs} are available in Tables S-1−S-4 (Supporting Information), while the second-order rate constants are summarized in Table 4.

Figure 3 and Figure S-3 (Supporting Information) show reaction 2 at 0.01 and 0.1 M ionic strengths. As shown in Table 4, the second-order rate constant decreases by about a factor of 2 at the higher ionic strength. Theoretically, ionic strength effects should obey the following equation:[23] $\log k = \log k_{ref} + 2z_Az_B[A\mu^{1/2}/(1 + \mu^{1/2})]$, where the value of A for acetonitrile at 25 °C is 1.646 $M^{-1/2}$.[3] This equation predicts that the reaction rate should be independent of ionic strength, given that the reductant is uncharged. The small observed dependence is attributed to a small degree of ion pairing for the cationic reactant. By way of comparison, a decrease by a factor of 10 is predicted for the anionic reductant in reaction 4.

(2) Reduction Kinetics Using $[Ru^{II}(hfac)_3]^-$. For reaction 4, as expected, both the forward and reverse reactions were found to obey second-order kinetics conforming to the differential rate expression

$$-d[Ru^{II}]/dt = k_{12}[Cu^{II}][Ru^{II}] - k_{21}[Cu^{I}][Ru^{III}] \qquad (14)$$

Experiments were performed at $\mu = 0.01$ M with excess $[Cu^{II}]$ (ranging from 0.025 to 0.175 mM) and $[Ru^{II}]_0 = 0.0025$ mM; $[Cu^{I}]$ (initial concentration: 0.0250 mM) was also at least 10-fold greater than $[Ru^{III}]$ (initial concentration: 0.000 mM). Under pseudo-first-order conditions eq 14 can be written as

$$-d[Ru^{II}]/dt = k_{12}'[Ru^{II}] - k_{21}'[Ru^{III}] \qquad (15)$$

where k_{12}' is $k_{12}[Cu^{II}]$ and k_{21}' is $k_{21}[Cu^{I}]$. Equation 15 leads to the following integrated expression:[23]

$$\ln\{([Ru^{II}] - [Ru^{II}]_\infty)/([Ru^{II}]_0 - [Ru^{II}]_\infty)\} = -k_{obs}t \qquad (16)$$

Here, k_{obs} represents $k_{12}' + k_{21}'$. The linear dependence of

(23) Espenson, J. H. *Chemical Kinetics and Reaction Mechanisms*; McGraw-Hill Book Co.: New York, 1981; pp 43, 172.

Table 4. Cross Reactions between $[Cu^{II}(bite)](BF_4)_2/[Cu^{I}(bite)](BF_4)$ and Selected Counter-Reagents[a]

reaction	reducing or oxidizing agents	K_{12}	k_{12} (M^{-1} s^{-1})	W_{12} (kcal mol^{-1})	f_{12}	k_{22} (M^{-1} s^{-1})	k_{11}[i] (M^{-1} s^{-1})
4	$[Ru^{II}(hfac)_3]^-$	2.18 ± 0.36[b]	$(8.22 \pm 0.27) \times 10^2$	1.02	1.00	$(4.3 \pm 0.2) \times 10^6$[f]	$(6.90 \pm 1.23) \times 10^{-2}$
1	$[Co^{II}((nox)_3(BC_6H_5)_2)]$	$(3.48 \pm 0.56) \times 10^8$[c]	$(3.70 \pm 0.11) \times 10^4$	1.54	0.149	272 ± 57[g]	$(4.09 \pm 2.05) \times 10^{-2}$
2	$[Co^{II}((nox)_3(BC_4H_9)_2)]$	$(2.29 \pm 0.37) \times 10^{10}$[c]	$(7.57 \pm 0.19) \times 10^4$[e]	1.54	0.065	132 ± 16[g]	$(1.19 \pm 0.24) \times 10^{-2}$
3	$[Co^{II}((dmg)_3(BC_4H_9)_2)]$	$(6.46 \pm 0.89) \times 10^{10}$[c]	$(7.40 \pm 0.29) \times 10^4$	1.54	0.054	546 ± 103[g]	$(1.22 \pm 0.29) \times 10^{-3}$
5	$[Fe^{III}(bpy)_3]^{3+}$	$(5.79 \pm 0.91) \times 10^5$[c,d]	$(2.50 \pm 0.06) \times 10^4$[d]	1.71	0.34	$(3.7 \pm 0.8) \times 10^6$[h]	$(2.94 \pm 0.79) \times 10^{-3}$[d]
							$\log k_{11,avg} = -2.17 \pm 0.80$

[a] In acetonitrile with 0.01 M Et_4NBF_4 at 25 °C except reaction 5 with 0.1 M Et_4NBF_4. [b] Equilibrium constant by pseudo-first-order kinetic method and spectrophotometric measurements. [c] Equilibrium constants by the equation $-nF\Delta E^\circ = -RT \ln K$ with $E_{1/2}$ for the Co(III/II) couples, Ru(III/II) couple, and Fe(III/II) couples as in Table 1 and $E_f = 320$ mV for $[Cu^{II/I}(bite)]^{2+/+}$ as derived from the equilibrium constant for reaction 4. [d] K_{21}, k_{21} (M^{-1} s^{-1}), $k_{11(Ox)}$ for reaction 5 of the oxidation of $[Cu^{I}(bite)]^+$. [e] $k_{12} = (3.97 \pm 0.06) \times 10^4$ M^{-1} s^{-1} at $\mu = 0.10$ M. [f] Reference 24. [g] Reference 9. [h] Reference 18. [i] Self-exchange rate constants by the Marcus Cross relationship as in eq 23.

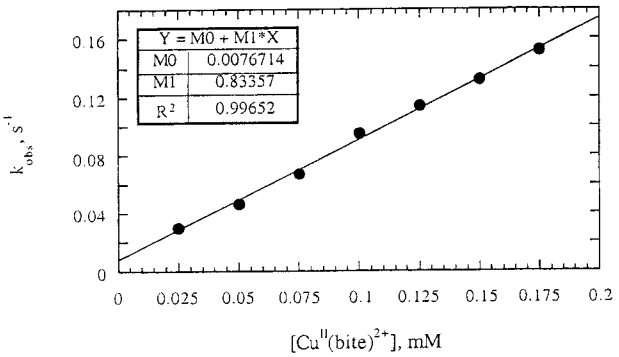

Figure 4. Pseudo-first-order rate constants for the reaction of $[Ru^{II}(hfac)_3]^-$ with excess $[Cu^{II}(bite)]^{2+}$ in acetonitrile with 0.01 M Et_4NBF_4 at 25 °C. $[Ru^{II}(hfac)_3^-]_0 = 0.0025$ mM. $[Cu^{I}(bite)^+]_0 = 0.0250$ mM.

k_{obs} on $[Cu^{II}]$ and $[Cu^{I}]$ implies eq 17:

$$k_{obs} = k_{12}[Cu^{II}] + k_{21}[Cu^{I}] \quad (17)$$

Seven different concentrations of oxidizing agent were used in the kinetic determinations and at least 10 determinations were carried out at each concentration, with data as shown for reaction 4 in Figure 4 and Table S-5 (Supporting Information). The slope and intercept of Figure 4 are k_{12} and $k_{21}[Cu^{I}]$, respectively, with k_{12} equal to $(8.22 \pm 0.27) \times 10^2$ M^{-1} s^{-1} and $k_{21}[Cu^{I}]$ equal to $(8.40 \pm 1.64) \times 10^{-3}$ s^{-1}. Therefore, k_{21} is $(3.36 \pm 0.66) \times 10^2$ M^{-1} s^{-1}.

The equilibrium constant for reaction 4 by the principle of detailed balancing is

$$K_{12} = k_{12}/k_{21} = 2.45 \pm 0.48 \quad (18)$$

Equilibrium constants for reaction 4 from this kinetic method and from the equilibrium spectrophotometric measurements are in excellent agreement with one another, the average equilibrium constant being given in Table 4.

(3) Oxidation Kinetics Using $[Fe^{III}(bpy)_3]^{3+}$. Reaction 5 was monitored by following the increase of absorbance due to $[Fe^{II}(bpy)_3]^{2+}$ at 522 nm. The kinetics were studied under pseudo-first-order conditions with at least a 10-fold excess of $[Fe^{III}(bpy)_3]^{3+}$. A higher ionic strength (0.1 M) was used because of electrolyte required in the electrolytic preparation of Fe(III). For the pseudo-first-order reaction 5, the integrated rate equation is of the form

$$\ln([Cu^{I}]_o/[Cu^{I}]_t) = k_{obs}t \quad (19)$$

where $[Cu^{I}]_o$ and $[Cu^{I}]_t$ represent the concentrations of $[Cu^{I}(bite)]^+$ at the time of reaction initiation and at any time, t, respectively. The kinetic data for reaction 5 are shown in Figure S-4 (Supporting Information). The linear dependence of k_{obs} on $[Fe^{III}]_o$ as in eq 20

$$k_{obs} = k_{21}[Fe^{III}]_o \quad (20)$$

indicates that, as expected, the reactions obey second-order kinetics conforming to the overall differential rate expression

$$-d[Fe^{III}]/dt = k_{21}[Cu^{I}][Fe^{III}] \quad (21)$$

At least 10 determinations were performed at each concentration. Values of k_{obs} are available in Table S-6 (Supporting Information), while the second-order rate constant is given in Table 4.

Discussion

The counter-reagents utilized in the cross-reaction kinetic studies were generally selected to promote an outer-sphere electron-transfer mechanism. The five reactions 1−5 investigated here for the $[Cu^{II/I}(bite)]^{2+/+}$ system fall in the class of one-electron complementary redox reactions. A one-electron outer-sphere electron-transfer mechanism is virtually assured by the well-established substitution-inert properties of the cobalt, iron, and ruthenium counter-reagents.

Equilibrium Constants. The equilibrium constant for reaction 4 has been determined by means of careful spectrophotometric measurements, defined as eq 10, and by pseudo-first-order kinetic determinations, shown in Figure 4 and eq 18. These results are in excellent agreement with one another. From the equilibrium constant for reaction 4, the formal potential for $[Cu^{II/I}(bite)]^{2+/+}$ can be derived by the equation

$$-nF\Delta E_f = -RT \ln K \quad (22)$$

where n is the number of electrons transferred, F is the Faraday constant, R is the gas constant, T is the absolute temperature, $\Delta E_f = E_{f(Ox)} - E_{f(Red)}$, and K is the equilibrium quotient. A value of $E_f = 320$ mVvs ferrocene/ferrocenium for $[Cu^{II/I}(bite)]^{2+/+}$ is obtained by use of $E_f = 300$ mV for $[Ru^{III/II}(hfac)_3]^{-/0}$ couple determined from CV. On the basis of this value of $E_f = 320$ mV for $[Cu^{II/I}(bite)]^{2+/+}$ and the reduction potentials for the counterreagents, the equilibrium quotients for reactions 1, 2, 3, and 5 have been calculated by using eq 22 and are listed in Table 4.

Apparent Self-Exchange Rate Constant. Self-exchange rate constants for many metal complexes in acetonitrile have been summarized by Wherland.[11] These include the cobalt clathrochelates and the ruthenium and iron complexes used in this work, although we have used the data as they appear in the

original literature source.[9,18,24] These self-exchange rate constants are given as k_{22} in Table 4 and were used in the calculation of the copper(II/I) self-exchange rate constants, k_{11}, by iterative solution of eq 23.

$$k_{11} = (k_{12})^2/[k_{22}K_{12}f_{12}(W_{12})^2] \quad (23)$$

Here, k_{12} is the second-order cross electron-transfer rate constant and K_{12} is the equilibrium constant. Equation 23 is a rearranged form of the Marcus cross relation,[25] which is usually given as

$$k_{12} = (k_{11}k_{22}K_{12}f_{12})^{1/2}W_{12} \quad (24)$$

The other terms (f_{12} and W_{12}) may be calculated from the relationships 25−29[25]

$$\ln f_{12} = \{[\ln K_{12} + (w_{12} - w_{21})/RT]^2\}/\{4[\ln(k_{11}k_{22}/Z^2) + (w_{11} + w_{22})/RT]\} \quad (25)$$

$$W_{12} = \exp[(-w_{12} - w_{21} + w_{11} + w_{22})/2RT] \quad (26)$$

$$w_{ij} = (Z_iZ_je^2)/(D_sa_{ij}(1 + \beta a_{ij}(\mu^{1/2}))) \quad (27)$$

In these equations, f_{12} is a nonlinear correction term, W_{12} is an electrostatic work term involved in bringing the reactants into outer-sphere contact, Z is taken as 1×10^{11} M^{-1} s^{-1}, a is the center-to-center distance in angstroms when the reactants are in contact, T is the absolute temperature, and R is the gas constant (in kilocalories). β is the ion interaction parameter given by[25]

$$\beta = ((8\pi Ne^2)/(1000D_skT))^{1/2} \quad (28)$$

where N is Avogadro constant 6.022×10^{23} mol^{-1}, e is the electronic charge, k is Boltzmann constant 1.38×10^{-23} J K^{-1}, and D_s is the static dielectric constant of the medium, 36.7 for acetonitrile at 25 °C.[26] These constants lead to the following expression for w_{ij} in acetonitrile at 25 °C:

$$w_{ij} = (9.05Z_iZ_j)/(a_{ij}(1 + 0.481a_{ij}(\mu^{1/2}))) \quad (29)$$

As estimated from CPK models, the average radius for the copper compounds is 5.7 Å, the average radius for the ruthenium compound is approximately 5.6 Å, the average radius for $[Fe^{III}(bpy)_3]^{3+}$ is approximately 6.8 Å, and the average radius for the three cobalt compounds is approximately 7.5 Å. The calculated values of W_{12} based on eqs 29 and 26 and of f_{12} based on eq 25 are shown in Table 4.

The second-order cross electron-transfer rate constants k_{12} from reactions 1−4 were obtained in acetonitrile with 0.01 M Et_4NBF_4 at 25 °C. Reaction 5 ($[Fe(bpy)_3]^{3+}$), on the other hand, was studied in the reverse direction (k_{21}) and at the higher ionic strength of 0.1 M. Despite these differences, the value of k_{11} derived from reaction 5 is bracketed by the values from the other four reactions. Apparently, the difference in ionic strength is compensated by the difference in charge type for reaction 5. The k_{11} values from all five cross-reactions are summarized in Table 4. They give a geometric mean of 1.05×10^{-2} M^{-1} s^{-1} for k_{11}. The k_{11} values in Table 4 span a range of a factor of 58, which is somewhat larger than normally encountered for simple outer-sphere electron-transfer reactions. The lowest value of k_{11} occurs for reaction 3 ($[Co^{II}((nox)_3(BC_4H_9)_2)]$), and it is the Co(II) reductant in this reaction that has $E°$ in disagreement with prior reports (as discussed above). As the literature value of k_{22} for this reagent was derived by application of the Marcus cross relationship and the value of $E°$ used in that calculation is questionable, we have reason to doubt the accuracy of the k_{11} value in Table 4 derived from reaction 3. A similar anomalous result was encountered in our prior study with this same reagent.[19] With the exclusion of reaction 3 the k_{11} values span the narrower range of a factor of 23, and the oxidation by $[Fe(bpy)_3]^{3+}$, reaction 5, yields a k_{11} value about 4-fold smaller than the value derived from reduction reaction 2. This difference is only of marginal significance.

Scheme 1

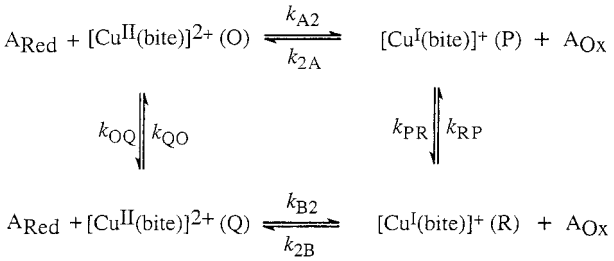

Square Scheme. Although our cross-reaction kinetic data do not require a complex mechanism, the combined X-ray crystallographic and ^1H NMR line-broadening data reported previously[5] strongly imply a sequential mechanism involving bimolecular electron-transfer and unimolecular isomerization steps. As we have discussed previously, X-ray crystallography shows that $[Cu^I(bite)]^+$ adopts a pseudo-tetrahedral structure with chirality at the copper center, at the two thioether sulfurs, and at the biphenyl linkage. Similar features pertain to $[Cu^{II}(bite)]^{2+}$, although there are conformational differences that lead to a pseudo-square-planar Cu(II) geometry. Both compounds, of course, are racemic. The relationship between the two structures is easily understood by comparing enantiomers of Cu(I) and Cu(II) that have the same chirality at the biphenyl linkage. In this comparison it is easy to see that the two structures differ in the chirality at both thioether sulfur atoms and that interconversion between the Cu(I) and Cu(II) structures can be achieved by inverting the two sulfur atoms. Alternatively, one might suppose that the biphenyl linkage could be inverted while retaining chirality at the sulfur centers, but CPK models show that the strain imposed by the macrocylic framework makes this process untenable. These considerations suggest that Cu(I) could undergo oxidation either by 1) isomerization from the stable pseudo-tetrahedral structure to a high-energy square-planar structure followed by electron transfer to generate stable square-planar Cu(II) or by 2) electron-transfer to generate unstable pseudo-tetrahedral Cu(II) followed by isomerization to stable square-planar Cu(II). The square scheme (with standard nomenclature)[7,27] shown in Scheme 1 illustrates these ideas.

Species O and R represent the stable forms of $[Cu^{II}(bite)]^{2+}$ and $[Cu^I(bite)]^+$, respectively, while species Q and P represent metastable intermediates. In principle, a ladder scheme could also arise,[28] since the two sulfur atoms could invert sequentially; however, as we have no evidence for this possibility it is not considered here.

(24) Chan, M.-S.; Wahl, A. C. *J. Phys. Chem.* **1982**, *86*, 126−130.
(25) *Inorganic Reactions and Methods*; Zuckerman, J. J., Ed.; VCH: Deerfield Beach, FL, 1986; Vol. 15, pp 13−47.
(26) Maryott, A. A.; Smith, E. R. *NBS Circular 514* **1951**, 1−7.
(27) Laviron, E.; Roullier, L. *J. Electroanal. Chem.* **1985**, *186*, 1−15.
(28) Villeneuve, N. M.; Schroeder, R. R.; Ochrymowycz, L. A.; Rorabacher, D. B. *Inorg. Chem.* **1997**, *36*, 4475−4483.

The overall differential rate expressions for the reduction of $[Cu^{II}(bite)]^{2+}$ and the oxidation of $[Cu^{I}(bite)]^{+}$ can be derived by adopting the steady-state approximation for the metastable intermediate species Q and P in Scheme 1. The resulting overall rate laws are as follows.[29]

For reduction:

$$-\mathrm{d}[Cu^{II}(bite)]/\mathrm{d}t = \left\{\frac{k_{A2}k_{PR}}{k_{A2}[A_{Ox}] + k_{PR}} + \frac{k_{B2}k_{OQ}}{k_{B2}[A_{Red}] + k_{QO}}\right\}[O][A_{Red}] \quad (30)$$

For oxidation:

$$-\mathrm{d}[Cu^{I}(bite)]/\mathrm{d}t = \left\{\frac{k_{A2}k_{RP}}{k_{A2}[A_{Ox}] + k_{PR}} + \frac{k_{B2}k_{OQ}}{k_{B2}[A_{Red}] + k_{QO}}\right\}[R][A_{Ox}] \quad (31)$$

The first and second terms in the brackets of each expression represent the kinetic contributions of rection via intermediates P and Q, respectively.

Equations 30 and 31 can lead to simple second-order rate laws under certain limiting conditions. When the reactions proceed via P and $k_{2A}[A_{Ox}] \ll k_{PR}$ the rate laws become

$$-\mathrm{d}[Cu^{II}(bite)]/\mathrm{d}t = k_{A2}[O][A_{Red}] \quad (32)$$

$$-\mathrm{d}[Cu^{I}(bite)]/\mathrm{d}t = (k_{RP}/k_{PR})k_{2A}[A_{Ox}][R] \quad (33)$$

And when the reactions proceed via Q with $k_{B2}[A_{Red}] \ll k_{QO}$ the second-order rate laws are

$$-\mathrm{d}[Cu^{II}(bite)]/\mathrm{d}t = (k_{B2}k_{OQ}/k_{QO})[O][A_{Red}] \quad (34)$$

$$-\mathrm{d}[Cu^{I}(bite)]/\mathrm{d}t = k_{2B}[R][A_{Ox}] \quad (35)$$

Under other conditions, isomerization can become rate limiting, yielding gated kinetics.

Rorabacher and co-workers have extensively documented that when the Marcus cross relationship is applied to electron-transfer reactions having second-order rate laws and proceeding via such a square scheme, inconsistencies can arise in the apparent self-exchange rate constants derived from oxidations and reductions.[7,30−32] Further discussion of this effect appears in the work of Koshino et al.[33−35] These inconsistences occur because some reactions go via intermediate Q while others go via P. On the other hand, it is simple to prove that such inconsistencies will not occur for systems where the microscopic electron-transfer rate constants obey Marcus theory and where both the oxidations and reductions go via the same intermediate. Moreover, when the real outer-sphere self-exchange reaction also proceeds via the same intermediate and with second-order kinetics, its rate constant should be the same as the apparent self-exchange rate constants derived from the cross reactions. Rorabacher et al. have described several examples of such systems.[31,36,37]

In the current study, the cross reactions have second-order rate laws indicative of nongated behavior. The apparent self-exchange rate constants obtained by applying the Marcus cross relationship to the experimentally determined cross-reaction rate constants are relatively constant for both oxidation and reduction reactions, which suggests that all of the cross reactions proceed through the same intermediate. By the above logic, if the second-order outer-sphere self-exchange rate constant were measurable it should be the same as the apparent self-exchange rate constant, 0.01 M^{-1} s^{-1}. The curious aspect of this system is that the real self-exchange reaction for $[Cu(bite)]^{2+/+}$ in acetone as studied by NMR line broadening does not obey second-order kinetics but has an overall first-order rate law, with rate $= k_{ex}[Cu^{I}(bite)^{+}]$ and $k_{ex} = 22$ s^{-1}.[5] Our inferred second-order self-exchange rate constant would give a pseudo-first-order rate constant for the self-exchange process of 8×10^{-6} s^{-1} under the typical conditions of 0.8 mM Cu(II). The fact that the real self-exchange reaction is many orders of magnitude faster than this suggests that it proceeds through an alternate mechanism or else that the observed NMR line-broadening is due to some process other than electron transfer. While we cannot completely discount the latter possibility, we believe, as shown below, that electron-transfer remains a viable explanation. In our prior work we proposed that the self-exchange reaction has a mechanism involving rate-limiting isomerization of Cu(I), followed by a fast outer-sphere electron-transfer process.[5] The reaction now appears to be more complex, perhaps proceeding through a mechanism with a rate-limiting change at Cu(I) followed by a fast inner-sphere electron-transfer step. Such an inner-sphere step might occur with a thiaether moiety dissociating from one redox center and binding to the other. Electron transfer via bridging thiaether ligands has been reported previously, for example in the dinuclear ruthenium ammine systems having bridging spirodithia-type ligands reported by Stein et al.[38]

This self-exchange mechanism can be represented as follows:

$$[Cu(bite)]^{+} \rightleftharpoons [Cu(bite^{*})]^{+} \quad k_1, k_{-1} \quad (36)$$

$$[Cu(bite^{*})]^{+} + [Cu(bite)]^{2+} \rightarrow [Cu(bite)]^{2+} + [Cu(bite^{*})]^{+} \quad k_{et} \quad (37)$$

Here, $[Cu(bite^{*})]^{+}$ represents an isomer of $[Cu(bite)]^{+}$ that is able to react with $[Cu(bite)]^{2+}$ through an inner-sphere mechanism, and the second step (eq 37) represents that inner-sphere process. This mechanism implies a nonsymmetric transition state, and since the reaction is degenerate there must also be a mirror-image transition state. With the application of the steady-state approximation to $[Cu(bite^{*})]^{+}$ the following rate law may be derived:

$$\text{rate} = \frac{2k_{et}k_1[Cu(bite)^{2+}][Cu(bite)^{+}]_{tot}}{(k_{et}[Cu(bite)^{2+}] + k_{-1})(1 + k_1/k_{-1})} \quad (38)$$

(29) Meagher, N. E.; Juntunen, K. L.; Salhi, C. A.; Ochrymowycz, L. A.; Rorabacher, D. B. *J. Am. Chem. Soc.* **1992**, *114*, 10411−10420.
(30) Vande Linde, A. M. Q.; Juntunen, K. L.; Mols, O.; Ksebati, M. B.; Ochrymowycz, L. A.; Rorabacher, D. B. *Inorg. Chem.* **1991**, *30*, 5037−5042.
(31) Vande Linde, A. M. Q.; Westerby, B. C.; Ochrymowycz, L. A.; Rorabacher, D. B. *Inorg. Chem.* **1993**, *32*, 251−257.
(32) Leggett, G. H.; Dunn, B. C.; Vande Linde, A. M. Q.; Ochrymowycz, L. A.; Rorabacher, D. B. *Inorg. Chem.* **1993**, *32*, 5911−5918.
(33) Koshino, N.; Kuchiyama, Y.; Funahashi, S.; Takagi, H. D. *Chem. Phys. Lett.* **1999**, *306*, 291−296.
(34) Koshino, N.; Kuchiyama, Y.; Ozaki, H.; Funahashi, S.; Takagi, H. D. *Inorg. Chem.* **1999**, *38*, 3352−3360.
(35) Koshino, N.; Kuchiyama, Y.; Funahashi, S.; Takagi, H. D. *Can J. Chem.* **1999**, *77*, 1498−1507.
(36) Dunn, B. C.; Ochrymowycz, L. A.; Rorabacher, D. B. *Inorg. Chem.* **1997**, *36*, 3253−3257.
(37) Dunn, B. C.; Wijetunge, P.; Vyvyan, J. R.; Howard, T. A.; Grall, A. J.; Ochrymowycz, L. A.; Rorabacher, D. B. *Inorg. Chem.* **1997**, *36*, 4484−4489.
(38) Stein, C. A.; Lewis, N. A.; Seitz, G. *J. Am. Chem. Soc.* **1982**, *104*, 2596−2599.

This rate law leads to kinetics independent of $[Cu(bite)^{2+}]$ when $k_{et}[Cu(bite)^{2+}]$ is much greater than k_{-1}. Koshino et al. have argued that gated self-exchange reactions with mechanisms formally equivalent to that in eqs 36 and 37 should always display second-order rate laws when measured by NMR line broadening methods,[34] and on this basis they have implied that our prior line-broadening results for the $[Cu(bite)]^{n+}$ system[5] must reflect some process other than the self-exchange electron-transfer reaction. Their argument was based on a mechanism analogous to ours (eqs 36 and 37), but their derived rate law differs from ours (eq 38) in that the denominator term in $[Cu(bite)^{2+}]$ is lacking. In view of the apparent error in the rate law derivation of Koshino et al., we see no inconsistency between our NMR rate law and an electron-transfer mechanism for line broadening.

Irrespective of the details of the self-exchange mechanism for $[Cu(bite)]^{2+/+}$, it is clear from the X-ray crystallography that the cross reactions should be interpreted in terms of a outer-sphere square scheme. Two phenomena that can be a consequence of a square scheme are transitions to first-order rate laws and to second-order rate laws proceeding via the alternate pathway. The NMR study of the self-exchange reaction suggests that the transition to first-order behavior should be observable in reactions of $[Cu(bite]^{+}$. Our efforts to test this suggestion in the reaction of $[Cu(bite)]^{+}$ with excess $[Fe(bpy)_3]^{3+}$ have been thwarted by solubility constraints that have made it impossible to study the reaction under conditions where k_{obs} might exceed 22 s^{-1}. Moreover, the fact that this 22 s^{-1} rate constant was obtained in acetone raises the possibility that the limiting rate constant might be significantly greater in aceetonitrile. The possibility of detecting limiting rates or a transition to the alternate pathway is a challenge for further research.

Conclusions

(1) The one-electron reduction of $[Cu^{II}(bite)]^{2+}$ by $[Ru^{II}(hfac)_3]^{-}$ proceeds to an equilibrium position, allowing the equilibrium constant to be determined by spectrophotometry. The equilibrium constant was also obtained from the kinetics. The results are consistent with one another.

(2) A square scheme is implied by the X-ray crystal structures and dynamic NMR results published previously.

(3) Five outer-sphere cross electron-exchange reactions obey second-order kinetics and give consistent self-exchange rate constants for $[Cu^{II/I}(bite)]^{2+/+}$ system with both oxidative and reductive reactions, despite the presumed operation of a square-scheme mechanism with $[Cu^{II/I}(bite)]^{2+/+}$ system. Apparently, all five reactions proceed through the same pathway.

(4) The derived self-exchange rate constant for $[Cu^{II/I}(bite)]^{2+/+}$ system is rather small, and it seems to imply that the more rapid exchange process seen by ^1H NMR line broadening reflects the intervention of an alternative mechanism.

Acknowledgment. Scott Flanagan (Rice University) is thanked for providing the samples of the $[Cu(bite)]^{2+}$ and $[Cu(bite)]^{+}$ salts. Professors Vince Cammarata (Auburn University) and Bill Henry (Mississippi State University) are thanked for their help in the electrochemical studies. Professors David Rorbacher (Wayne State University), Scot Wherland (Washington State University), and Mike Weaver (Purdue University) are thanked for their helpful comments. Professor Fred Anson (Caltech) is thanked for graciously acting as a sabbatical host to D.M.S. during the preparation of this manuscript; he is also thanked for providing access to DigiSim. A portion of this research was funded by an NSF grant (D.M.S.) and a grant from the Robert A. Welch Foundation (L.J.W.).

Supporting Information Available: Tables S-1−S-6, giving values of k_{obs}. Figures S-1−S-4, showing plots of k_{obs} vs [excess reagent] for reactions 1, 3, and 2 (at $\mu = 0.1$ M) and 5, respectively. This material is available free of charge via the Internet at http://pubs.acs.org.

IC000358W